Quantitative analysis of temperature effects in radiation damage of thiolate-based self-assembled monolayers

2006 J. Phys.: Condens. Matter 18 S1677

(http://iopscience.iop.org/0953-8984/18/30/S15)

INSTITUTE OF PHYSICS PUBLISHING JOURNAL OF PHYSICS: CONDENSED MATTER

J. Phys.: Condens. Matter **18** (2006) S1677–S1689 doi:10.1088/0953-8984/18/30/S15

Quantitative analysis of temperature effects in radiation damage of thiolate-based self-assembled monolayers

A Shaporenko[1], **M Zharnikov**[1,4], **P Feulner**[2,4] **and D Menzel**[2,3]

[1] Angewandte Physikalische Chemie, Universität Heidelberg, Im Neuenheimer Feld 253, D-69120 Heidelberg, Germany
[2] Physikdepartment E20, Technische Universität München, D-85747 Garching, Germany
[3] Fritz-Haber-Institut der MPG, Faradayweg 4-6, D-14195 Berlin, Germany

Received 16 February 2006, in final form 14 March 2006
Published 14 July 2006
Online at stacks.iop.org/JPhysCM/18/S1677

Abstract

Following our earlier finding of temperature effects in the radiation damage of self-assembled monolayers (SAMs) we investigated in detail the x-ray-induced modification of aliphatic and aromatic thiolate-based SAMs formed from dodecanethiol and biphenylthiol on gold substrates as representative test systems. For six sample temperatures between 50 and 300 K we measured cross sections and saturation behaviour for the most prominent irradiation-induced reactions, including desorption of hydrocarbon fragments, breaking of the headgroup–substrate bond, and formation of cross-linking networks and secondary bonds of the headgroup atoms within the layer. The results are discussed.

1. Introduction

The effect of ionizing radiation on organic materials, biological macromolecules, and cells is an important issue with wide practical significance both in everyday life and in science. Useful model systems for the understanding of the complex processes important in these effects are self-assembled monolayers (SAMs). These are close-packed arrays of amphiphilic molecules, in which the headgroup of an adsorbate covalently bonds to a solid substrate, while the chainlike molecular tail sticks out from the substrate [1–3]. In addition, the irradiation-induced modifications of SAMs are also interesting in their own right, in view of lithographic applications of these systems [4–13] and the possible influences of radiation damage during their characterization by x-ray- and electron-based techniques (see e.g. [14, 15]).

According to previous work [16–32], exposure of SAMs to ionizing radiation results in a series of complex, strongly interrelated processes, including the loss of orientational and conformational order, partial dehydrogenation, formation of a cross-linking network between

[4] Corresponding authors.

the SAM-constituents, desorption of film fragments and individual molecules, and damage of the headgroup–substrate interface. So far, mostly electron-induced modification of SAMs has been investigated, both qualitatively and quantitatively [17, 21–25, 28, 29, 32]. In particular, cross-sections of several major irradiation-induced processes for SAMs of alkanethiolates (ATs) [21, 22, 28] and semifluorinated alkanethiolates [29] have been obtained, and details of the microscopic processes have been investigated [22]. No quantitative data on x-ray-induced modification of SAMs are available, even though several qualitative studies of the respective phenomena have been carried out [16, 18–20, 28, 30, 31]; however, it will turn out that the photon-induced effects are similar to those caused by primary electrons and the actual photon energies used are not very important, agreeing with and corroborating earlier conclusions that the predominant excitation source are the secondary electrons. In recent publications [33, 34] we have shown that strong temperature effects exist in some of the consequences of irradiation but not in others: those processes which are connected with the mobility of large fragments are efficiently quenched at cryogenic temperatures while those due to local rearrangement and atom desorption persist even there.

In the present paper, we present and analyse first *quantitative* results on the modification of SAMs by soft x-rays, and give a detailed analysis of the temperature dependences. As test systems, we selected films of alkanethiolates and biphenylthiolates on gold, which are good representatives of the major classes of SAMs. Our aims are (i) to look in detail at the temperature dependence of the various effects going stepwise from cryogenic to room temperature and (ii) to compare the results for aliphatic films with those for aromatic ones.

In the following section we describe the experimental procedure and techniques. The results are presented and briefly discussed in section 3. An extended analysis of the data is given in section 4 followed by a summary in section 5.

2. Experimental set-up

The experiments were performed at the 49II-PGM-I beamline of the synchrotron radiation facility BESSY II in Berlin. SAMs of dodecanethiol ($CH_3(CH_2)_{11}SH$, C12) and biphenylthiol (C_6H_5–C_6H_4–SH, BPT) [35] were prepared *ex situ* by immersion of Au substrates for 24 h into 1 mM solution of the respective substances in ethanol (C12) and DMF (BPT), with subsequent rinsing and drying. The substrates were 300 nm of gold evaporated either onto titanium-primed polished single-crystal Si(100) wafers, or onto mica substrates; the resulting Au films were polycrystalline, with predominant (111) orientation. After the preparation, we transferred the samples into a UHV system with a base pressure of 3×10^{-9} Pa for characterization and irradiation. In UHV, the samples could be cooled to less than 50 K with l-He, and heated by thermal radiation from a tungsten filament mounted behind them. Their temperature was measured with a chromel/alumel thermocouple pressed onto one corner of their surface by a molybdenum spring. We have monitored x-ray and secondary electron induced damage by x-ray absorption spectroscopy (XAS), photoemission (PE), and desorption induced by electronic transitions (DIET) of neutrals. DIET of neutrals was measured with a highly sensitive quadrupole mass spectrometer. In the latter, efficient background suppression was maintained by cryo- and titanium sublimation pumping of the mass spectrometer's ionizer region, and by chopping the synchrotron light and applying lock-in detection (see [36] for details). PE spectra were obtained with a hemispherical analyser equipped with a fivefold channeltron detector for enhanced sensitivity, and XAS data with a standard partial electron yield (PEY) detector. All spectra were normalized to the photon flux. A quantitative investigation of radiation damage requires the determination of absolute photon exposures. We obtained the photon flux from the photocurrent of a type-calibrated GaAsP Schottky diode [37], and the beam area from the photocurrent of a knife edge which was swept vertically and horizontally through the beam.

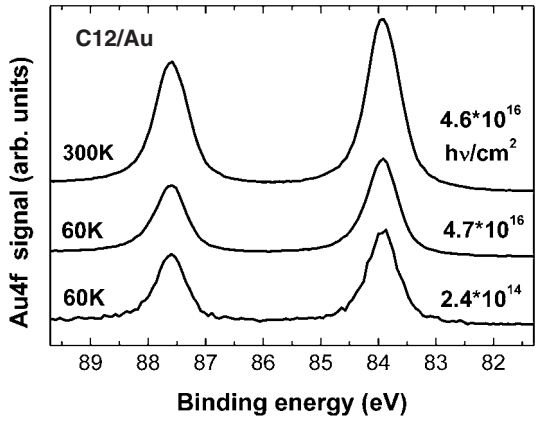

Figure 1. Au 4f PE spectra of minimally (bottom curve) and extensively irradiated C12/Au ($h\nu = 260$ eV). Prolonged irradiation was performed at 60 K (centre curve) and 300 K (top curve). A dose of 2.4×10^{14} $h\nu$ cm^{-2} was delivered during the spectrum acquisition, which is quite low at 60 K, so that the bottom spectrum is representative for the pristine film.

On the basis of these calibration procedures, we were able to obtain the absolute values of photon exposures accurate within a factor of two (corresponding to an interval of $-50\%/+100\%$). The exposure dependence of irradiation damage was obtained from consecutively recorded PE and XAS spectra with photon energies between 250 and 350 eV. Within this energy range, we found only minor changes of the overall damage rate as a function of photon energy. This is in agreement with previous results which identified excitations by secondary electrons mainly from the substrate as the main sources of irradiation effects [10, 16, 18, 30, 38]. Similar results have been obtained for x-ray stimulated desorption of neutral particles from thin condensed films [39].

3. Results

As mentioned in section 1, exposure of SAMs to ionizing radiation results in loss of the orientational and conformational order, partial dehydrogenation, formation of cross-linking networks between the SAM constituents, desorption of film fragments and individual molecules, and damage of the headgroup–substrate interface. Most of these processes contain complex reaction scenarios, including bond breaking, transport of fragments and their desorption, or formation of new bonds inside the layer. The monitoring of all these individual reaction steps is quite difficult. So far, only the dehydrogenation process by electron impact has been studied in detail [22]. It is, however, possible to monitor characteristic parameters which can be considered as integral fingerprints of the complex, multi-step processes. One of these parameters is the extent of irradiation-induced desorption, which mostly consists of hydrocarbon fragments [14, 28, 32–34], since the desorbing hydrogen atoms and molecules [21, 22] do not carry noticeable mass.

To evaluate the extent of overall irradiation-induced desorption, we monitored the intensity of the Au 4f XPS lines originating from the substrate, during continuous irradiation of C12 and BPT samples with 260 and 350 eV photons, respectively. As an illustration of the observed effects, Au 4f spectra of pristine (bottom curve, radiation dose only that necessary for the spectrum) and extensively irradiated C12/Au are presented in figure 1 for two different irradiation temperatures, 60 and 300 K (similar traces were obtained for the BPT samples).

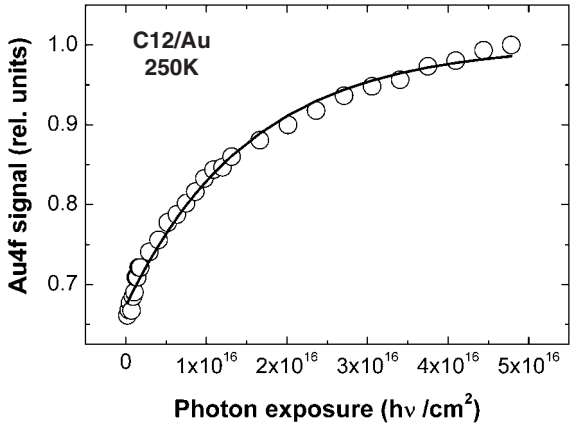

Figure 2. Au 4f intensity as a function of photon exposure ($h\nu = 260$ eV; circles, experimental data; full line, fit by the exponential function according to equation (1)). Similar fit qualities have been obtained for BPT/Au.

For the sample kept at 300 K during the exposure to x-rays, we observe a noticeable increase in the Au 4f intensity caused by x-ray irradiation, due to reduced attenuation of the substrate signal by the thinner (because of irradiation-induced desorption) hydrocarbon film. The respective intensity increase occurs at 60 K as well but at a much lower rate, so that the corresponding changes are almost invisible in figure 1.

Taking the entire spectrum series for every particular temperature, the extent and rate of the irradiation-induced desorption at each temperature can be derived from the fitting of the dose dependence of the Au 4f intensity with a simple exponential function

$$I = I_{\text{sat}} + (I_{\text{pris}} - I_{\text{sat}}) \times \exp(-\sigma \Phi / S_{\text{irrad}}), \tag{1}$$

where I is the intensity value in a course of irradiation, I_{pris} and I_{sat} are the intensity values for the pristine and strongly irradiated film (a levelling off behaviour), respectively, Φ is the cumulative photon exposure, S_{irrad} is the area irradiated by the x-ray beam, and the cross section σ (expressed here in cm^2/photon) is a measure of the process rate. An example of such a fit is given in figure 2 for C12/Au and $T = 250$ K.

Combining the results for different temperatures, we obtain the temperature dependence of the cross-section for the irradiation-induced removal of material (figures 3(a), (b)). Utilizing data on primary film thickness and mean free path of electrons in these layers [40], we also extract the saturation values of material loss after extended irradiation as a function of the sample temperature from the fit (figures 4(a), (b)).

The cross sections for photon induced reduction of the film thickness are quite large and not very different for both types of SAMs, even though slightly lower for BPT/Au. We obtain 2×10^{-17} cm^2 at our lowest sample temperatures for C12 ($h\nu = 260$ eV) as well as for BPT SAMs ($h\nu = 350$ eV; note that the photon energy has only minor influence on the radiation damage). These values increase with increasing sample temperatures, by a factor of five at room temperature for C12 and by a factor of three for BPT. We note that these room temperature values are only about one order of magnitude smaller than the geometric cross sections of these molecules.

The saturation behaviour, on the other hand, is very different for aliphatic and aromatic SAMs. Prolonged irradiation with 260 (350) eV photons at room temperature decreases the thickness of the C12 layers by 40%, but that of the BPT SAMs only by 10%. At lower

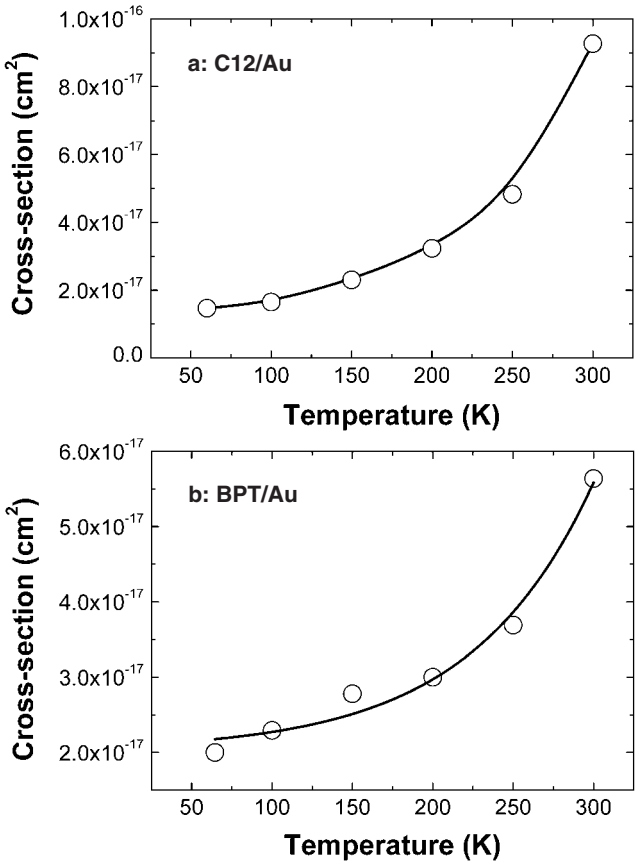

Figure 3. ((a), (b)) Cross-sections σ of x-ray-irradiation-induced desorption for C12 (a) and BPT SAMs (b) as a function of temperature (solid lines: averaged trend to guide the eye).

temperatures much less material can be removed by irradiation, for C12 as well as for BPT (figures 4(a), (b)). We note that the saturation values obtained here for room temperature are in perfect agreement with previous experiments, where C12 and BPT layers have been irradiated with electrons [10, 28]. This is not surprising as secondary electrons are believed to be the main source of irradiation damage even in the case of exposure to photons [16, 18, 30].

From the above results we see that cryogenic conditions help to minimize material loss considerably. The sensitivity of the cross sections *and* the saturation values of thickness reduction to temperature indicates that different reaction types prevail at low and high temperatures. Previous PSD experiments have shown desorption of *large* fragments at room temperature, but only desorption of *small* fragments with not more than three C atoms at 50–60 K. This behaviour has been identified for SAMs prepared by hydrosilylation on Si [33, 34], for aliphatic SAMs on diamond surfaces [41], for phosphonate-coupled SAMs on native silicon oxide [42], and for thiolate-bonded alkanes on Au and Ag substrates (see as an example the mass spectra for C12/Ag in figure 5). We therefore regard the respective temperature effect as a general phenomenon for radiation damage in thin organic films. XAS (x-ray absorption spectroscopy) data from C16/Au [33, 34] indicate formation of double bonds due to hydrogen abstraction as well as the loss of orientational and conformational order, also in agreement with

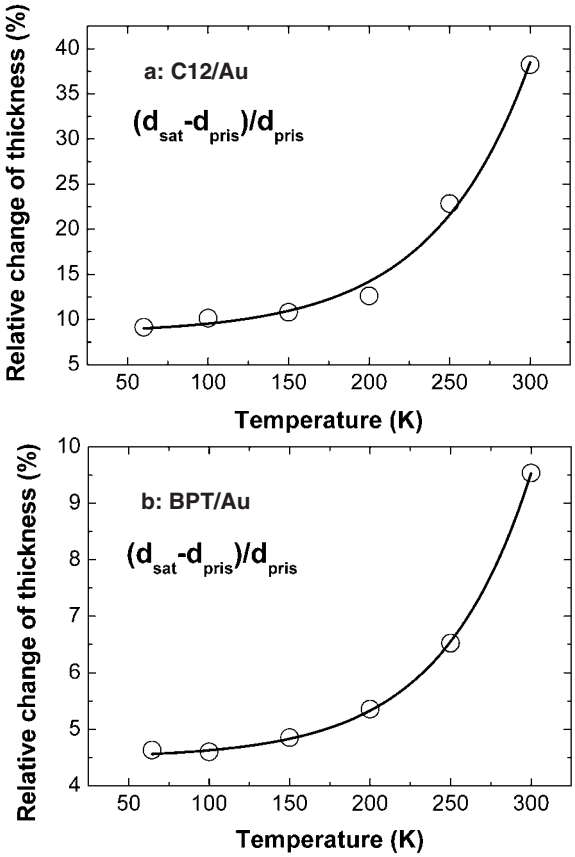

Figure 4. ((a), (b)) Saturation values for the relative (%) reduction of the layer thickness by extended irradiation as a function of the sample temperature, for C16/Au (a) and BPT/Au (b) (solid lines: averaged trend to guide the eye).

previous electron irradiation investigations [18, 21, 22, 28]. The cross section of double bond formation has been found to be much less dependent on temperature (by a factor of about 1.5 on going from 50 to 300 K) than those for irradiation-induced desorption, a further hint that temperature effects get smaller for small fragments.

A further class of reactions finally concerns the headgroup–substrate interface. Two different reaction pathways have been determined for the exposure of thiolate-bound SAMs to ionizing radiation: (i) breaking of the thiolate–carbon bond and accumulation of atomic sulfur at the surface [33, 34, 43], and (ii) breaking of the thiolate bond, movement of the entire S–C_xH_y chain from the surface, and formation of dialkylsulfide species [30]. For aliphatic SAMs on Au reaction type (ii) was shown to predominate by far at room temperatures; at 50 K, the contributions of both processes (i) and (ii) were comparable [33]. In our present study, we take a more quantitative look on the temperature dependence of these electronically stimulated processes, and also include BPT samples in consideration. We do this by analysing S 2p PE data as shown in figures 6(a) and (b) as a function of sample temperature and photon exposure.

Contributions from the three different S species with S $2p_{3/2}$ binding energy positions at 162.0 eV (pristine thiolate species [44, 45]), 163.2 eV (dialkylsulfide [44]) and 161.0 eV (atomic S [46]) are clearly discernible, for the aliphatic as well as the aromatic SAMs (compare

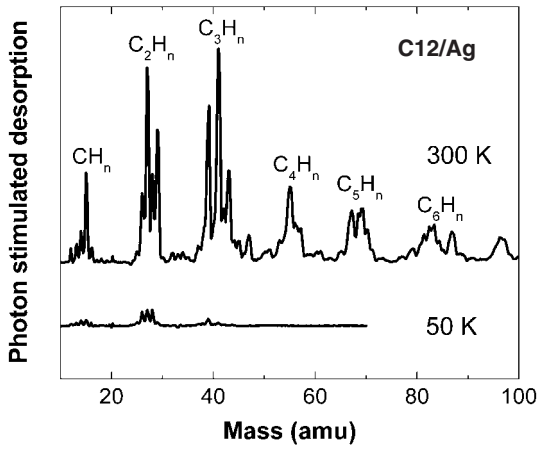

Figure 5. Mass distribution of desorbing neutrals in the case of x-ray ($h\nu = 260$ eV) stimulated desorption from C12/Ag at 51 and 300 K.

figures 6(a) and (b); for BPT we use the term 'sulfide species' for the R–S–R′ entities because in this case R and R′ will not be pure alkyl radicals). By fitting these spectra with pseudo-Voigt functions we extracted the areas of the respective S $2p_{3/2,1/2}$ doublets and fitted their dose dependence at each temperature by the simple exponential function according to equation (1) to obtain cross-section values for the beam damage of the headgroup–substrate interface. The results for the R–S–R′ species, which is the main reaction product (see figures 6 and 8), are plotted in figures 7(a) and (b).

By comparing figures 7(a) and (b) with figures 3(a) and (b), it becomes obvious that the cross sections for x-ray irradiation-induced desorption and for sulfide production as well as their temperature dependences are almost identical within the scatter of our experiment. Figures 8(a) and (b) show the evolution of the sulfur-derived species for C12/Au and BPT/Au layers (after irradiation with 5×10^{16} photons cm^{-2} in each case) as a function of the sample temperature. The curves indicate that thiolate loss and sulfide build-up are mirror images of each other. The atomic S, which is a minority species for both samples (and is close to the detection limit for BPT/Au), *in*creases with *de*creasing temperature, i.e. behaves oppositely to the other effects.

We note that there is also an alternative assignment for the sulfur S 2p doublet at 161.0 eV (S $2p_{3/2}$): instead of ascribing it to atomic sulfur as mentioned, a change of the bonding of the sulfur atom compared to thiolate, without breaking of the C–S bond, has been inferred. This assignment is based on kinetic studies of the SAM formation: the doublet at ≈161.0 eV was observed to appear at the early stage of the molecular assembly, i.e. for a short immersion time, and disappear later [47–49]. Our experiments do not allow us to favour one of the two assignments in the present case, since both breaking of the C–S bond and build-up of another bond between the headgroup sulfur and metal substrate are possible under irradiation. However, since low coverages with lying chains are the prerequisite of this different type of sulfide, which is not attained under our conditions, we believe that the explanation by atomic S is the more likely one here.

4. Discussion

In accordance with previous results (see references in section 1), we can distinguish different types of irradiation stimulated reactions.

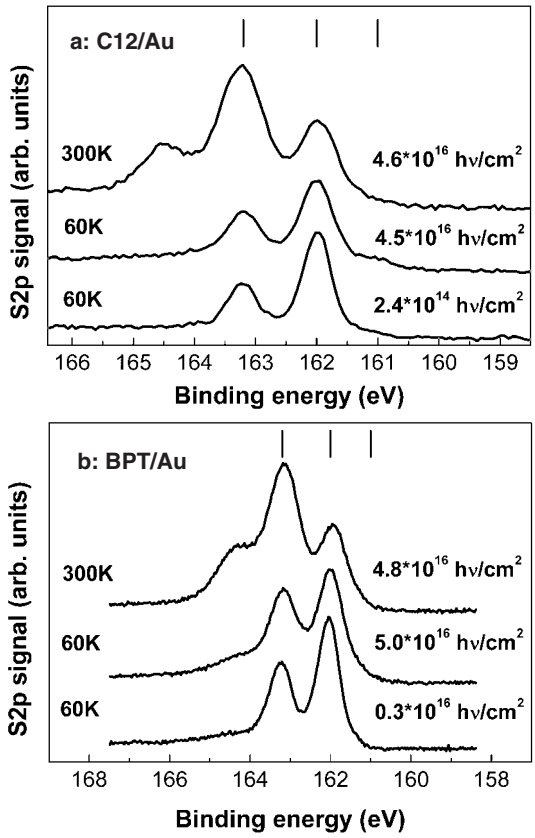

Figure 6. S 2p PE spectra of pristine (bottom curves) and extensively irradiated C12/Au (a) and BPT/Au (b). The irradiation was performed at 60 K (middle curve) and 300 K (top curve). Doses of 2.4×10^{14} $h\nu$ cm^{-2} (C12, $h\nu = 260$ eV) and 3×10^{15} $h\nu$ cm^{-2} (BPT, $h\nu = 350$ eV) were delivered during the spectrum acquisition and are quite low at 60 K, so that the bottom spectra are representative for the pristine films. The S $2p_{3/2}$ positions of the three different contributions (see the text) are marked.

(1) Formation of differently bound or atomic sulfur on the gold surface (by breaking of the bond between the S headgroup and the alkyl chain).
(2) Breaking of the thiolate–Au bond, movement of the entire S-alkyl (S-biphenyl) chain or at least a large part R of it from the surface and formation of secondary R–S–R′ sulfide bonds within the SAM.
(3) Loss of material, i.e. desorption of hydrocarbon fragments and entire molecules.
(4) Abstraction of hydrogen and formation of free radicals and unsaturated bonds, which is a prerequisite for the formation of cross-linking network and the above sulfide reaction.
(5) Loss of orientational order and formation of a cross-linking network between the partially dehydrogenated SAM constituents as monitored by NEXAFS [10, 33, 34].

(A sixth type of reaction, namely selective damage of the endgroup at the vacuum interface, is beyond the capabilities of the currently applied analytical tools. It requires the application and evaluation of highly resolved XAS data, which will be presented in a forthcoming publication.)

Reaction (1), namely the formation of atomic S, is obviously in competition with reaction (2): the increase of sulfide formation at higher temperatures decreases the source for atomic S,

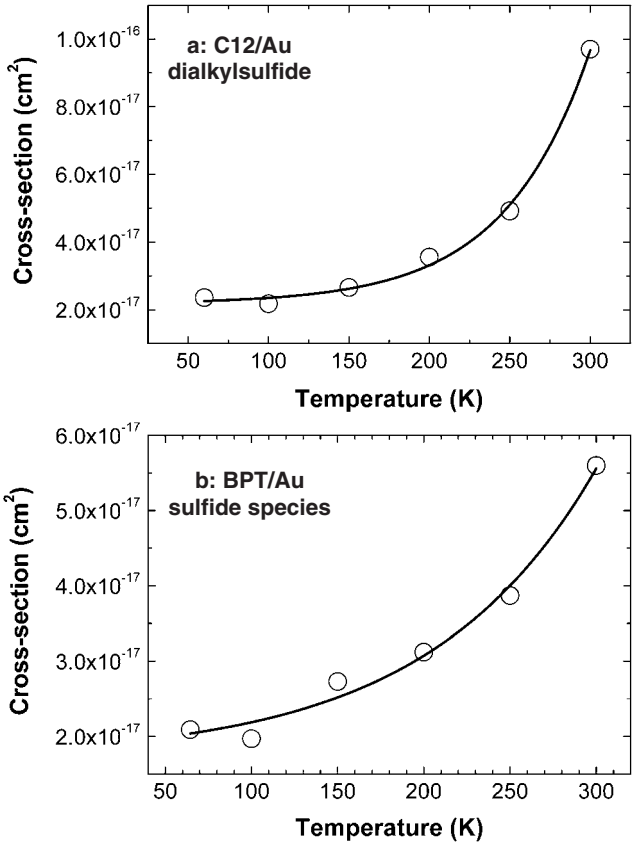

Figure 7. ((a), (b)) Cross sections for x-ray-irradiation-induced formation of sulfide species as a function of temperature for C12/Au (a) and BPT/Au (b). Solid lines: averaged trend to guide the eye.

which explains its decrease with increasing T. However, it is much less probable than (2) for all sample temperatures investigated here. The relative increase of differently bound or atomic S at cryogenic conditions is due to the hindrance of (2) at low temperatures (figure 8(a)). For BPT/Au the concentration of atomic S is so low that the unambiguous discrimination of its temperature dependence is impossible from our data. We draw the tentative conclusion that within the experimental scatter the temperature dependence of reaction (1) results exclusively from the temperature dependence of reaction (2), i.e. the loss of intact thiolate bonds (which is necessary for the first reaction) by irradiation at elevated temperature. Reactions (2) and (3) have in common that both are promoted by elevated sample temperatures, whereas the temperature dependence of reaction (4) is very weak. The fact that the cross sections of reaction (2) and that for the integral material loss (3) are practically equal for a wide temperature range and two different types of samples (cf figures 3(a), (b) and 7(a), (b)) is surprising and suggests that both reactions are governed by the same factors. Considering only the above data for C12 and BPT on Au one could draw the conclusion that an identical primary step exists for (2) and (3), which would likely be the rupture of the headgroup–substrate bond. This explanation, however, is ruled out by data of electron beam damage comparing Ag and Au based SAMs which show identical values for the material loss as a function of the electron exposure at

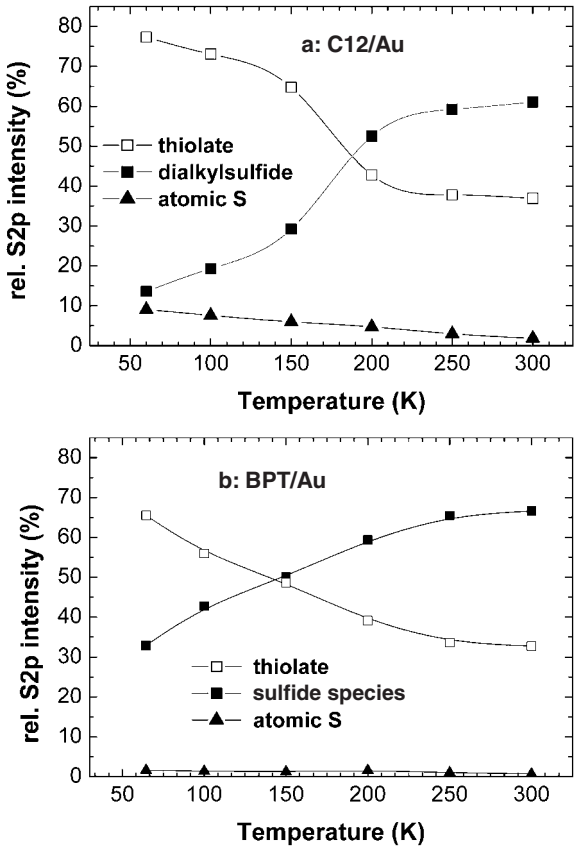

Figure 8. ((a), (b)) Proportions of the individual sulfur-derived species after irradiation of C12/Au (a) and BPT/Au (b) with 5×10^{16} photons cm^{-2} at a definite temperature (solid lines to guide the eye). The values were obtained from the S 2p XPS spectra.

room temperature, but very different yields for the R–S–R′ reaction [28], probably because of the stronger S-to-metal bond for Ag than for Au [1–3]. Instead we have to look for thermally activated *intermediate* processes in the multi-step scenario of beam damage which the two reactions (2) and (3) have in common. Diffusive transport of entire chains or larger fragments of them obviously is such a process. Di-R-sulfide formation requires that hydrocarbon chains having lost their anchoring at the metal diffuse away from the substrate in order to form sulfide bonds with unsaturated bonds created by hydrogen abstraction. Rapid material loss at room temperature, on the other hand, is brought about by desorption of large chain fragments as clearly indicated by the mass spectrometric data for a large variety of systems (see figure 5 and examples mentioned there). Without diffusive transport of these large fragments towards the vacuum interface this reaction type would not exist. We therefore assume diffusive transport as the key thermally activated process which reactions (2) and (3) have in common.

Unfortunately an Arrhenius analysis of the temperature dependence of the cross sections of (2) and (3) fails. Compared with a simple Arrhenius law, the cross section values obtained by us (figures 3(a), (b); 7(a), (b)) are too large at low temperatures, and too small at high temperatures. This could be explained by assuming a temperature independent pedestal for both reaction rates, and contributions of different channels with different activation energies.

Although such a scenario is likely in view of the very different fragment masses encountered (compare figure 5), an unambiguous modelling of the transport processes and their temperature dependence on the basis of the present data is impossible. Further experiments with soft ionization techniques particularly on the fragmentation behaviour are mandatory (we note that the data in figure 5 have not been corrected for fragmentation by electron impact in the ionizer of the mass spectrometer, simply because reliable data on fragmentation of large radicals were not available; large fragments and parent molecules are underestimated in figure 5, therefore).

Beam damage of C12/Au and BPT/Au exhibits saturation behaviour (figures 4(a) and (b)). In particular, the integral material loss (i.e. the desorption of large fragments and entire molecules) levels off at 40% for C12/Au and 10% for BPT/Au. This saturation behaviour is related to the formation of double bonds indicated by the appearance of the characteristic [C 1s]π^* resonance at 285.0 eV [10, 14, 18, 33], and by the formation of a cross-linking network between neighbouring SAM constituents, which is fingerprinted by an increase in the etching resistance of the aromatic thiols [24]. These modifications stabilize the layers against further radiation attack, probably by supporting rapid delocalization of the electronic excitation, and by cross-linking. If this radiation induced blocking of beam damage did not exist no saturation behaviour could be expected. Moreover, the successive loss of neighbours should ease diffusion and 'autocatalytically' accelerate the beam damage reaction, which is not observed.

The observed difference between the absolute values of the integral material loss at saturation in C12/Au and BPT/Au is related to a higher efficiency of the cross-linking processes in the latter system due to a higher stability of the aromatic backbones as compared to the aliphatic ones [10, 24]. Note once more that the absolute values of the integral material loss at saturation, obtained in the present work for the case of x-ray irradiation, practically coincide with the analogous values for the case of electron irradiation [10, 28]. This is further evidence that the effect provided by soft x-rays on SAMs is predominantly mediated by the secondary electrons originated from the metal substrate, which has much higher electron yield than the hydrocarbon matrix of the SAMs (see [22, 32] for a survey of bond breaking mechanisms by slow electrons).

We note that diffusion is a thermally activated process, whereas electronically stimulated hydrogen abstraction does not measurably depend on the SAM temperature. As a result, hindrance by cross-linking will win over diffusion mediated beam damage for low temperatures already at low exposure values, as verified by the data displayed in figures 4(a) and (b) and 8(a) and (b).

The fact that mass spectrometric data show very similar temperature behaviour for a large variety of organic thin films on metal, semiconductor and insulator substrates points to very similar microscopic scenarios for all of these samples. We believe that the above sketched scenario of competition between thermally stimulated diffusive transport of large fragments and eventually also of entire molecules, and blocking by radiation induced intermolecular bonds, applies to a large class of materials. At low temperature only those channels survive which do not depend on transport of large hydrocarbon fragments, e.g. abstraction and desorption of hydrogen [22] and small fragments. If our explanation holds, freezing of the structure, i.e. hindrance of diffusive transport by low sample temperatures, is the predominant reason for cryo-mediated radiation hardening of thin organic films, as is generally assumed in the field of cryomicroscopy [50]. The microscopic processes by which cooling quenches beam damage are however not simple, as shown above. The primary aspect of cooling is the reduction of the transport rate by which large fragments created by irradiation-induced chain rupture can proceed towards desorption. It reduces the rate of material loss at given photon flux. A second aspect is that non-activated processes which are in competition with activated processes are

favoured by cryogenic conditions. Cross-linking is such a non-activated process in our example. Its support by low temperature causes accelerated saturation of the beam induced material loss. Finally, we find that the creation of R–S–R′ species is quenched by low temperatures. From a mechanistic point of view, this is certainly the most interesting point. It simply means that rupture of the headgroup–metal bond can only be completed if the hydrocarbon chain is sufficiently mobile. We emphasize that the excitation rate of antibonding states of this complex, which is the first step in electronically induced bond breaking, is certainly temperature independent, i.e. the trial frequency will be the same at low and high temperatures. At low temperature, however, the cage effect imposed by the surrounding hydrocarbon matrix keeps the headgroup at its site and favours rebonding. This is a clear example that cryogenic conditions can support healing of radiation damage.

5. Conclusions

Our detailed temperature-dependent results for the efficiency of radiation induced total removal of SAMs, of the formation of sulfide groups in the SAM–Au interface, and of the build-up of atomic S in the interface have corroborated the semiquantitative findings of our earlier report. Data for C12 as well as for BPT SAMs have been obtained. The first two effects increase strongly with temperature while the third one, which is much smaller, varies oppositely, which can be explained by assuming that disulfide does not form atomic S. The fluence dependences, which have been measured at six temperatures between 50 and 300 K, can be represented by first order rates with saturation values, so that absolute desorption and conversion cross sections can be determined and their temperature dependence demonstrated. While the cross sections are similar for the first two effects and for both types of SAMs, the saturation values are quite different for the two types, with maximum effects much smaller for BPT. These saturation values are interpreted by cross-linking of the chains by irradiation. The strong temperature dependences for the effects which necessitate movement of large fragments or entire chains is likely due to diffusive motion of the latter which is facilitated by increased temperatures. However, an Arrhenius interpretation of the temperature dependences fails, which probably means that there are other mechanisms than diffusion. The information accessible to us now does not warrant further interpretation at present.

Acknowledgments

We thank K Eberle, R Schneider, M Glanz, and the staff of BESSY, in particular W Braun, H Pfau, and O Schwarzkopf for help during the experiments and M Grunze for support of this work. Financial support by the BMBF (05 KS4VHA/4 and 05 ES3XBA/5) is gratefully acknowledged.

References

[1] Ulman A 1991 *An Introduction to Ultrathin Organic Films: Langmuir–Blodgett to Self-Assembly* (New York: Academic)
Ulman A 1996 *Chem. Rev.* **96** 1533
[2] Schreiber F 2000 *Prog. Surf. Sci.* **65** 151
[3] Love J C, Estroff L A, Kriebel J K, Nuzzo R G and Whitesides G M 2005 *Chem. Rev.* **105** 1103
[4] Lercel M J, Redinbo G F, Pardo F D, Rooks M, Tiberio R C, Simpson P, Craighead H G, Sheen C W, Parikh A N and Allara D L 1994 *J. Vac. Sci. Technol.* B **12** 3663
[5] Xu S and Liu G 1997 *Langmuir* **13** 127
[6] Maoz R, Cohen S R and Sagiv J 1999 *Adv. Mater.* **11** 55

[7] Brandow S L, Chen M S, Aggarwal R, Dulcey C S, Calvert J M and Dressick W 1999 *Langmuir* **15** 5429
[8] Gölzhäuser A, Geyer W, Stadler V, Eck W, Grunze M, Edinger K, Weimann T and Hinze P 2000 *J. Vac. Sci. Technol.* B **18** 3414
[9] Gölzhäuser A, Eck W, Geyer W, Stadler V, Weimann T, Hinze P and Grunze M 2001 *Adv. Mater.* **13** 806
[10] Zharnikov M and Grunze M 2002 *J. Vac. Sci. Technol.* B **20** 1793
[11] Fuierer R, Carroll R L, Feldheim D L and Gorman C B 2002 *Adv. Mater.* **14** 154
[12] Kim S O, Solak H H, Stoykovich M P, Ferrier N J, de Pablo J J and Nealey P F 2003 *Nature* **424** 411
[13] Klauser R, Hong I H, Huang M L, Wang S C, Chuang T J, Terfort A and Zharnikov M 2004 *Langmuir* **20** 2050
[14] Zharnikov M and Grunze M 2001 *J. Phys.: Condens. Matter* **13** 11333
[15] Duwez A S 2004 *J. Electron. Spectrosc. Relat. Phenom.* **134** 97
[16] Laibinis P E, Graham R L, Biebuyck H A and Whitesides G M 1991 *Science* **254** 981
[17] Seshadri K, Froyd K, Parikh A N, Allara D L, Lercel M J and Craighead H G 1996 *J. Phys. Chem.* **100** 15900
[18] Jäger B, Schürmann H, Müller H U, Himmel H-J, Neumann M, Grunze M and Wöll Ch 1997 *Z. Phys. Chem.* **202** 263
[19] Wirde M, Gelius U, Dunbar T and Allara D L 1997 *Nucl. Instrum. Methods Phys. Res.* B **131** 245
[20] Frydman E, Cohen H, Maoz R and Sagiv J 1997 *Langmuir* **13** 5089
[21] Olsen C and Rowntree P A 1998 *J. Chem. Phys.* **108** 3750
[22] Garand E and Rowntree P A 2005 *J. Phys. Chem.* B **109** 12927
[23] Zerulla D and Chasse T 1999 *Langmuir* **15** 5285
[24] Geyer W, Stadler V, Eck W, Zharnikov M, Gölzhäuser A and Grunze M 1999 *Appl. Phys. Lett.* **75** 2401
[25] Eck W, Stadler V, Geyer W, Zharnikov M, Gölzhäuser A and Grunze M 2000 *Adv. Mater.* **12** 805
[26] Chenakin S P, Heinz B and Morgner H 1999 *Surf. Sci.* **421** 337
[27] Hutt D A and Leggett G J 1999 *J. Mater. Chem.* **9** 923
[28] Zharnikov M, Frey S, Heister K and Grunze M 2000 *Langmuir* **16** 2697
[29] Frey S, Heister K, Zharnikov M and Grunze M 2000 *Phys. Chem. Chem. Phys.* **2** 1979
Frey S, Heister K, Zharnikov M and Grunze M 2000 *Phys. Chem. Chem. Phys.* **2** 3721 (erratum)
[30] Heister K, Zharnikov M, Grunze M, Johansson L S O and Ulman A 2001 *Langmuir* **17** 8
[31] Wagner A J, Carlo S R, Vecitis C and Fairbrother D H 2002 *Langmuir* **18** 1542
[32] Huels M A, Dugal P C and Sanche L 2003 *J. Chem. Phys.* **118** 11168
[33] Feulner P, Niedermayer T, Eberle K, Schneider R, Menzel D, Baumer A, Schmich E, Shaporenko A, Tai Y and Zharnikov M 2004 *Phys. Rev. Lett.* **93** 178302
[34] Feulner P, Niedermayer T, Eberle K, Schneider R, Menzel D, Baumer A, Schmich E, Shaporenko A, Tai Y and Zharnikov M 2005 *Surf. Sci.* **593** 252
[35] Frey S, Stadler V, Heister K, Eck W, Zharnikov M, Grunze M, Zeysing B and Terfort A 2001 *Langmuir* **17** 2408
[36] Romberg R, Frigo S P, Ogurtsov A, Feulner P and Menzel D 2000 *Surf. Sci.* **451** 116
[37] Kummrey M, Tegeler E, Barth J, Krisch M, Schäfers F and Wolf R 1988 *Appl. Opt.* **27** 4336
[38] Zharnikov M, Frey S, Gölzhäuser A, Geyer W and Grunze M 1999 *Phys. Chem. Chem. Phys.* **1** 3163
[39] Wada S, Matsumoto Y, Kohno M, Sekitani T and Tanaka K 2004 *J. Electron Spectrosc. Relat. Phenom.* **137–140** 211
[40] Lamont C L A and Wilkes J 1999 *Langmuir* **15** 2037
[41] Schmich E 2004 *Diploma Thesis* Technische Universität München
[42] Neppl S *et al* 2005 unpublished
[43] Kondoh H and Nozoye H 1998 *J. Phys. Chem.* B **102** 2367
[44] Heister K, Zharnikov M, Grunze M and Johansson L S O 2001 *J. Phys. Chem.* B **105** 4058
[45] Laibinis P E, Whitesides G M, Allara D L, Tao Y-T, Parikh A N and Nuzzo R G 1991 *J. Am. Chem. Soc.* **113** 7152
[46] Yang Y-W and Fan L-J 2002 *Langmuir* **18** 1157
[47] Ishida T, Hara M, Kojima I, Tsuneda S, Nishida N, Sasabe H and Knoll W 1998 *Langmuir* **14** 2092
[48] Himmelhaus M, Gauss I, Buck M, Eisert F, Wöll Ch and Grunze M 1998 *J. Electron. Spectrosc. Relat. Phenom.* **92** 139
[49] Ishida T, Choi N, Mizutani W, Tokumoto H, Kojima I, Azehara H, Hokari H, Akiba U and Fujihira M 1999 *Langmuir* **15** 6799
[50] See, e.g. Cosslett V E 1978 *J. Microsc.* **113** 113
Schneider G 1994 *X-Ray Microscopy IV* ed V V Aristov and A I Erko (Chernolgolovka: Bogorodskii Pechatnik) p 181